iJRASET
International Journal For Research in Applied Science and Engineering Technology

INTERNATIONAL JOURNAL FOR RESEARCH

IN APPLIED SCIENCE & ENGINEERING TECHNOLOGY

Volume: 12 **Issue:** IV **Month of publication:** April 2024

DOI: https://doi.org/10.22214/ijraset.2024.59765

www.ijraset.com

Call: 08813907089 | E-mail ID: ijraset@gmail.com

International Journal for Research in Applied Science & Engineering Technology (IJRASET)
ISSN: 2321-9653; IC Value: 45.98; SJ Impact Factor: 7.538
Volume 12 Issue IV Apr 2024- Available at www.ijraset.com

Enhancement of X-Ray Images by Gradient Domain Guided Filtering and Non Sub Sampled Shearlet Transform

G. Rajesh Babu[1], J. Jaya Durga[2], Sk. Abdul Khadar[3], Ch. Hemani[4], N. V. V. Seshu Babu[5]
[1]*Dept. of ECE, Usha Rama College of Engineeringand Technology, Telaprolu, Unguturu Mandal, Krishna, Andhra Pradesh, India*
[2, 3, 4, 5]*B.Tech Students, Dept. of ECE, Usha Rama College of Engineering and Technology,Telaprolu, Unguturu Mandal, Krishna, Andhra Pradesh, India*

Abstract: ***In order to address the issues of low resolution, noise amplification, missing details, and weak edge gradient retention in the X-ray image improvement process, we propose in this study an image enhancement technique that combines non-Subsampled Shearlet transform with gradient-domain guided filtering. We start by breaking down the non Subsampled Shearlet transform and histogram equalization into the original image. We receive multiple high-frequency sub-bands as well as a low-frequency sub-band. To enhance the overall contrast of the image and bring out the contour information in the low-frequency sub-band, adaptive gamma correction with weighting distribution is applied. To reduce image noise and emphasize edge information and detail, gradient-domain guided filtering is applied to the high-frequency sub-bands. In order to generate the final enhanced image, we use the inverse non-Subsampled Shearlet transform to reconstruct all of the sub-bands that were successfully processed. The experimental findings demonstrate the effectiveness of the suggested algorithm in improving X-ray images, as well as the clear advantages its objective index provides over certain conventional algorithms.***

Keywords: image enhancement, histogram equalization, non-Subsampled Shearlet transform, gradient-domain guided filtering, X-ray image.

I. INRODUCTION

With advancements in photoelectric detecting and image analysis technologies, X-ray images are now often used in medical diagnosis, security inspection, aerospace, defect detection, machinery manufacture, and other industries. Low dynamic range, low definition, low contrast, and excessive noise are present in the X-ray instrument's image, the hardware equipment's image, and the detecting principle of the radiographic inspection system. The acquired image is used directly for defect detection and image analysis. The detection results become noticeably inaccurate as a result. Therefore, it is advantageous to analyze X-ray images using image enhancement techniques [1,2], as this improves image quality and visual effects and facilitates subsequent detection. The most popular image enhancement algorithms are spatial domain pixel enhancement and transform domain multi-scale coefficient improvement enhancement techniques. Through pixel-by-pixel processing techniques including histogram equalization [3,4,5], image sharpening and grayscale stretching [6,7,8], and retinex theory [9], the spatial domain can be improved. A gray-level information histogram for X-ray image contrast enhancement was proposed by Zeng et al. [10], and it significantly enhances the performance of several histogram-based enhancement algorithms. But, there will be an over-enhancement issue that results in distorted images when an image is enhanced. Nonlinear unsharp masking was first presented for mammography enhancement by Panetta et al. [11]. When it comes to bringing out the small features in the original photographs, this method works well. But at the same time, it overshoots the crisp details and amplifies noise. A retinex-based framework for improving medical X-ray images was presented by Tao et al. [12]. The dark area pixels in the original image distort the contour borders of the image, showing shadows that never were. Despite this, the framework can improve details, reduce noise, and increase contrast.

The original image is transformed into the frequency domain for multi-scale decomposition first, and then the enhanced image is inversely transformed after amplifying or filtering the decomposed sub-image. Frequently employed transformations include the wavelet transform [13], ridgelet transform [14], curvelet transform [15], wedgelet transform [16], contourlet transform [17], nonsubsampled contourlet transform (NSCT) [18,19], Shearlet transform [20,21], nonsubsampled Shearlet transform (NSST) [22], and others. An approach to improve the details at various scales in screening mammography was presented by Tang et al. [23] and was based on a multiscale measure in the wavelet domain.

Wavelet transform, however, is not very good at capturing anisotropic singular features in images since it can only record data in three directions: horizontal, vertical, and diagonal. An intensity adaptive nonlinear multiscale detail and contrast enhancement method was proposed by Ostojié et al. [24] for digital radiography. The technique adjusts to the local exposure level, which lessens the saliency of the artifacts; nonetheless, the detail improvement adaption to image pixel intensity has to be reinforced. A medical image enhancement technique based on enhanced gamma correction in the Shearlet domain was presented by Zhou et al. [25]. This technique greatly improves overall contrast and highlights the image's textural features. However, because this approach lacks translation invariance, the picture will result in a pseudo-Gibbs phenomena.

Images following NSST may achieve optimal sparse representation and nonlinear error approximation due to the unconstrained shearing directions. Numerous successes have been made while using the NSST for image enhancement. In order to improve blur, Zhang et al. [26] used NSST and tetrolet transform on remote sensing photos, successfully preserving the image's edges and details while greatly enhancing the information entropy and mean. Li et al. [27] investigated the NSST domain. The pseudo-Gibbs phenomenon is successfully eliminated from the image during the enhancement process by the contrast enhancement method, which leverages the remote sensing image enhancement coefficient as an adjustable pattern recognition job. A phase stretching transformation and NSST-based visual sensor image enhancement technique was presented by Tong et al. [28]. In this approach, the author processes the various scale components following NSST decomposition using nonlinear models with various thresholds. The algorithm has the ability to reduce noise and successfully boost the image's contrast. The parameter selection has some degree of randomness, and none of the aforementioned research have examined the parameters and effects of the NSST's shearing orientations and decomposition levels.

A linear edge-preserving guided image filtering technique was proposed by He et al. [29]. Detailed information won't be blurred in the filtered image. In order to solve the issue of abiding by halo artifacts, Li et al. [30] proposed a weighted guided image filter by adding an edge-aware weighting into an already-existing guided image filter. In order to lessen the impact of image edge smoothing, Kou et al. [31] suggested gradient-domain guided filtering and added first-order edge-aware restrictions to image processing, which can better maintain image edges. However, edge retention may be decreased and edges may be too smoothed when intensity domain limitations are applied to edges and details. We suggest an image enhancing technique to deal with the aforementioned problems. It is applied to X-ray pictures and is based on gradient-domain guided filtering and NSST. The approach combines gradient-domain guided filtering for enhancing picture detail with the benefits of NSST for sparse image representation. The low-frequency sub-band highlights minute details in the background by boosting contrast using adaptive gamma correction with a weighted distribution. By evaluating the image quality of the four-levels direction decomposition under various scale decomposition levels and the image quality of different direction decomposition sequences under the four-levels scale decomposition, the high-frequency sub-bands use gradient-domain guided filtering to remove image noise and extract edge and texture information. In order to determine the ideal NSST decomposition parameters, we compare the execution times of several decompositions. The suggested approach may produce high-quality images for further research and analysis by enhancing the contrast, details, and texture information of medical and industrial X-ray images, as demonstrated by the enhancement experiments conducted on these images.

II. RELATED WORK

A. *Non Subsampled Shearlet Transform*

Non Subsampled Shearlet transform (NSST) is a kind of non Subsampled multiscale transform, which was introduced based on the theory of Shearlet transform [11]. The image is decomposed by NSST into multiple scales with multiple directions by multiscale and multidirectional decompositions. Firstly, the nonsubsampled pyramid (NSP) is adopted as the multiscale decomposition filter to decompose the image into one low-frequency sub-band and one high-frequency sub-band. Then, the high-frequency sub-band is decomposed by the shearing filter (SF) to achieve the multidirectional sub-bands. Due to the NSST decomposition process having no subsampling for the NSP and the SF, the NSST is shift-invariant. Its construction is simple and anisotropic, and in dimension n = 2, the affine systems with composite dilations are collections of the form:

$$\Lambda_{AB}(\psi) = \left\{ \psi_{j,l,k}(x) = |\det A|^{j/2} \psi(B^l A^j x - k) : j,l \in \mathbb{Z}, k \in \mathbb{Z}^2 \right\}$$

$$A = \begin{pmatrix} a & 0 \\ 0 & \sqrt{a} \end{pmatrix}, B = \begin{pmatrix} 1 & s \\ 0 & 1 \end{pmatrix} \quad (1)$$

A is a 2-dimensional invertible matrix of anisotropic expansion, which is related to scale transformation. B is a 2-dimensional shear invertible matrix, related to rotation or shear transformation, and |detA| = 1, j, l, k represents the scale parameter, shearing parameter, and translation parameter. This synthetic wavelet is called a shear wave when a = 4, s = 1. As shown in Figure 1, the three-levels NSST decomposition structure diagram, in which the scale parameter j = 3 and the numbers of the shearing parameters of each level are set to [2–4] respectively, then the corresponding shearing directions of each level are [4,8,16].

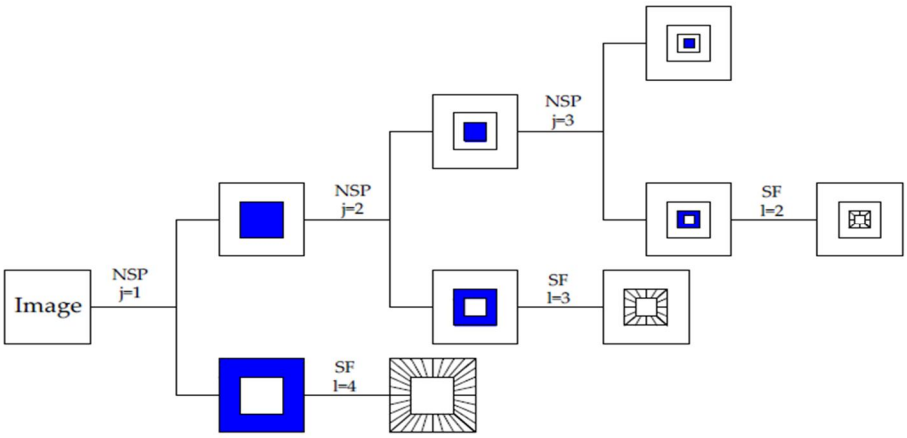

Fig.1 Three level NSST decomposition process

B. Adaptive Gamma Correction with Weighted Distribution

Gamma correction can expand the bright part in the X-ray image to make the image contrast more obvious, and the simple form of the transform-based gamma correction is derived by equation (2).

The gamma correction on an image I is defined as follows:

$$T(l) = l_{max}\left(\frac{l}{l_{max}}\right)^{\gamma} = l_{max}\left(\frac{l}{l_{max}}\right)^{1-cdf(l)} \quad (2)$$

The AGC method can progressively increase the low intensity and avoid the significant decrement of the high intensity. Furthermore, the weighting distribution (WD) function is also applied to slightly modify the statistical histogram and lessen the generation of adverse effects . The WD function is formulated as:

$$pdf_w(l) = pdf_{max}\left(\frac{pdf(l)-pdf_{min}}{pdf_{max}-pdf_{min}}\right)^{\alpha} \quad (3)$$

where α is the adjusted parameter, pdf_{max} is the maximum pdf of the statistical histogram, and pdf_{min} is the minimum pdf . Based on Equation (3), the modified cdf is approximated by:

$$cdf_w(l) = \sum_{l=0}^{l_{max}} \frac{pdf_w(l)}{\sum_{l=0}^{l_{max}} pdf_w(l)} \quad (4)$$

Based on the value of cdf, the value of gamma is modified as follows:

$$\gamma = 1 - cdf_w(l) \quad (5)$$

Since most of the pixels of the X-ray image are densely distributed in the low grayscale area, the AGCWD algorithm can gradually increase the low pixel intensity of the image based on the weight distribution function, smooth the fluctuation phenomenon, and thus reduce the excessive enhancement of the image by gamma correction.

C. Gradient Domain Guided Filtering

The output of any pixel in the filtered image can be expressed as the following linear model:

$$Z(p) = a_{p'}G(p) + b_{p'} \qquad \forall p \in \Omega_r(p') \quad (6)$$

Among them, Z(p) is the output image, G(p) is the guidance image. $\Omega_r(p')$ is a local square window with the point p′ as the center and r as the radius in the guide image G(p). $a_{p'}$ and $b_{p'}$ are the constant term coefficients in the window $\Omega_r(p')$. The values of $a_{p'}$ and $b_{p'}$ are calculated from the following equation.

$$E = \sum_{p\in\Omega_{s_1}(p')} [(a_{p'}G(p) + b_{p'} - X(p))^2 + \frac{\lambda}{\hat{\Gamma}_{G(p')}}(a_{p'} - \gamma_{p'})^2] \quad (7)$$

Among them, X(p) is the image to be filtered, λ is the regularization parameter to prevent $a_{p'}$ from being too large, and $\hat{\Gamma}_{G(p')}$ is the edge perception weight, which is defined as follows:

$$\hat{\Gamma}_{G(p')} = \frac{1}{N}\sum_{p=1}^{N}\frac{\chi(p')+\varepsilon}{\chi(p)+\varepsilon}$$
$$\chi(p') = \sigma_{G,1}(p') \times \sigma_{G,\varsigma 1}(p') \quad (8)$$

Where $\sigma_{G,1}(p')$ is the standard deviation within the window 3x3 and $\sigma_{G,\varsigma 1}(p')$ is the standard deviation within the window 2r +1 x 2r +1 centered on the point p′. ε is defined as $(0.001XL)^2$where L is the dynamic range of input image. To minimize the noise of the filtered image, take the minimum value of E, and the linear regression is used to solve the formula (7) to obtain

$$a_{p'} = \frac{\mu_{G\odot X,\varsigma 1}(p') - \mu_{G,\varsigma 1}(p')\mu_{X,\varsigma 1}(p') + \frac{\lambda}{\hat{\Gamma}_{G(p')}}\gamma_{p'}}{\sigma^2_{G,\varsigma 1}(p') + \frac{\lambda}{\hat{\Gamma}_{G(p')}}}$$
$$b_{p'} = \mu_{X,\varsigma 1}(p') - a_{p'}\mu_{G,\varsigma 1}(p') \quad (9)$$

When the above values are substituted in the formula of Z(p), the final formula of Z(p) is given below:

$$Z(p) = \overline{a_p}G(p) + \overline{b_p} \quad (10)$$

Where $\overline{a_p}$, $\overline{b_p}$ are the mean values of $a_{p'}$, $b_{p'}$ in the window $\Omega_r(p')$.

Gradient-domain guided filtering preserves its detailed features while smoothing the image. To further enhance the edge and texture information of the image, the smoothed image is subtracted from the original image to obtain a different image, which is added to the smoothed image to obtain an enhanced image.

III. PROPOSED ALGORITHM

The block diagram of proposed method is shown in figure 2. The high-frequency subbands of the image contain noise, and as the decomposition scale increases, they become almost invisible. We use gradient-domain guided filtering to process the high-frequency sub-bands to reduce noise interference. The detailed information in the image can be well preserved. To display the high-frequency images more clearly, both the high-frequency subbands and the images enhanced by the gradient domain guided filtering have undergone a linear grayscale transformation.

1) *Step 1:* Perform histogram equalization on the X-ray image, stretch the overall grayscale range of the image, and improve the image layering.
2) *Step 2:* Perform NSST scale decomposition on the image processed in Step 1 to obtain one low-frequency sub-band and multiple high-frequency sub-bands.

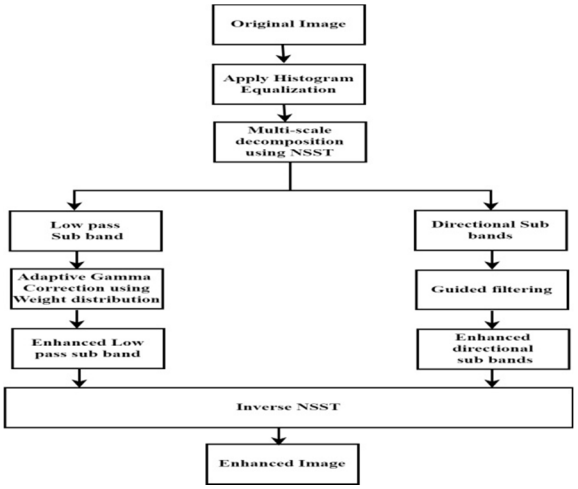

Fig.2 Image enhancement using proposed method

3) *Step 3:* Use adaptive gamma correction with weighted distribution to enhance the contrast of the low-frequency sub-band to highlight a small amount of detailed information in the background.
4) *Step 4:* Use gradient-domain guided filtering for the high-frequency sub-bands to filter out image noise and subtract the smoothed image from the original image to obtain a differential image, which was added to the smoothed image to perform image enhancement.
5) *Step 5:* Perform inverse NSST on the processed low-frequency sub-band and high frequency sub-bands and output the final enhanced image.

A. Effect of decomposition levels of NSST on image enhancement

The key parameters of NSST decomposition are the decomposition levels and shearing directions of each level. To analyze the effect of decomposition levels on image quality five X-ray images of different sizes and different grayscales were selected for the experiments.

For the X-ray Image with the size of 440 x 440, The enhanced X-ray images obtained under different decomposition levels are shown in Figure 3, where (a) is the original image, and (b–f) corresponds to the decomposition levels j equal to 1–5.

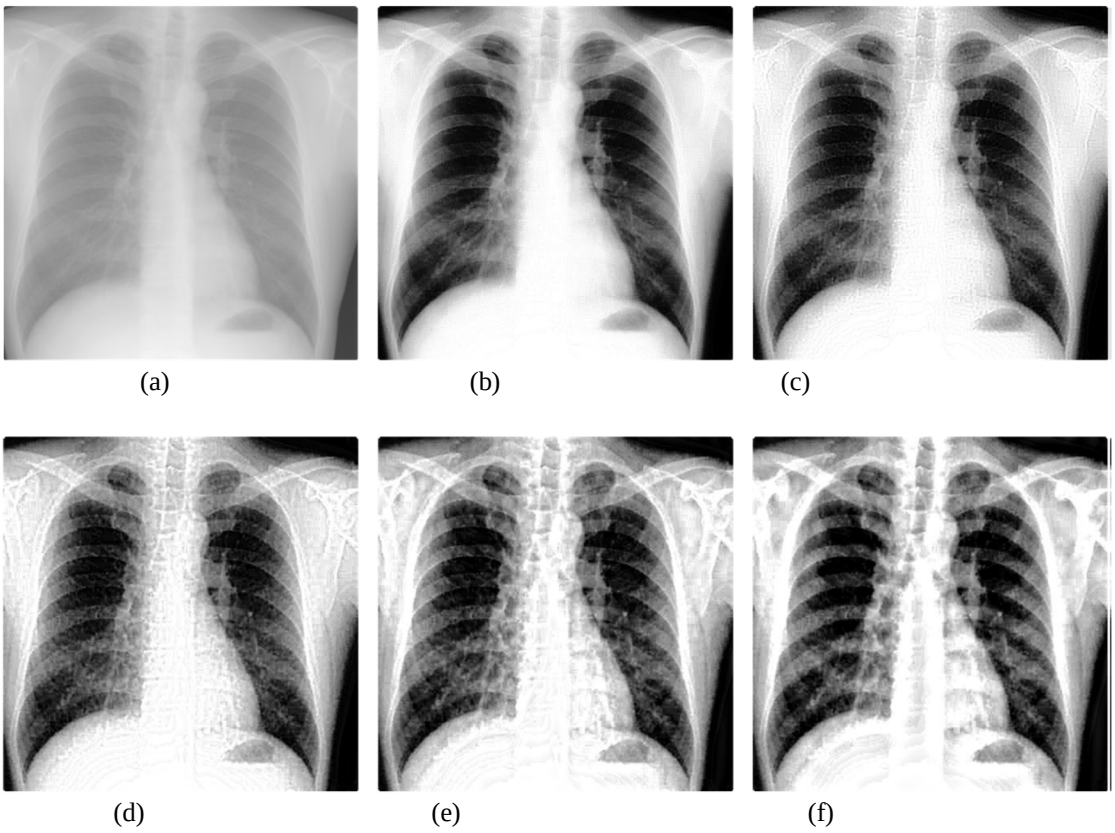

Fig.3 Effect of decomposition levels of NSST on X-ray image of 440x440 size

When the decomposition scale $j < 3$, with the increase of the NSST decomposition scale, the boundary and texture features of the image are gradually obvious, and the detailed information is enhanced. When $5 > j > 3$, the enhancement effect is further improved; the change is not significant. For the X-ray Image with the size of 1024 x 1024, The enhanced X-ray images obtained under different decomposition levels are shown in Figure 4, where (a) is the original image, and (b–f) corresponds to the decomposition levels j equal to 1–5.

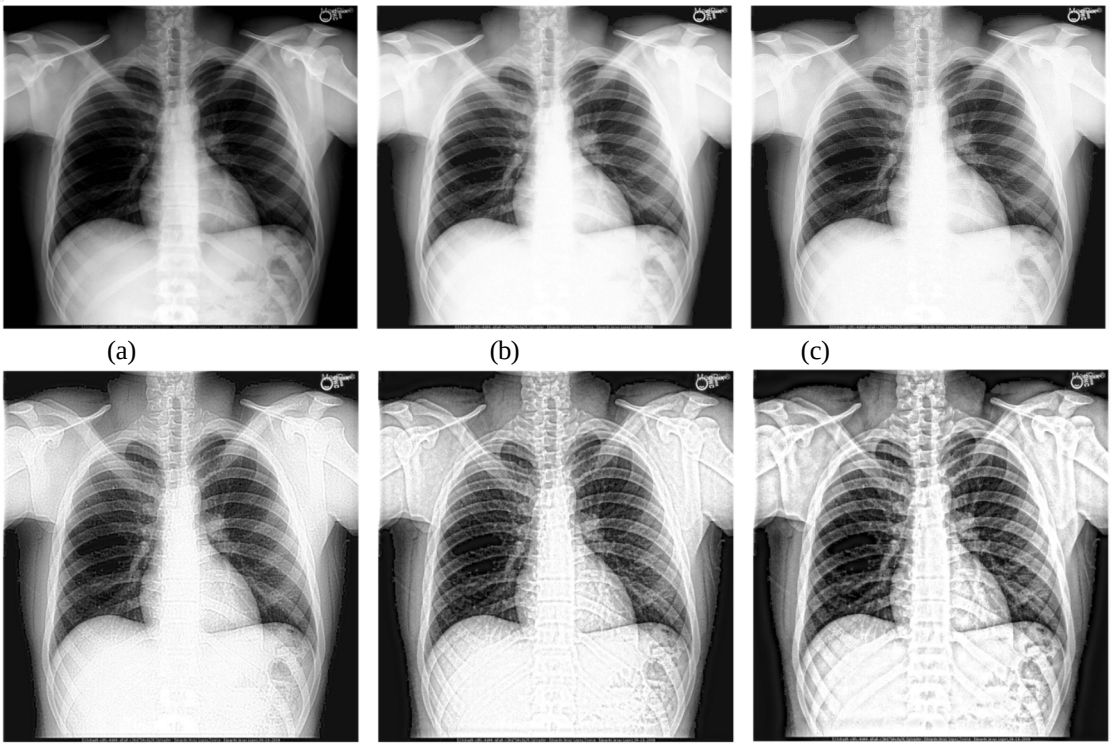

(a) (b) (c)

(d) (e) (f)

Fig.4 Effect of decomposition levels of NSST on X-ray image of 1024x1024

When the decomposition scale j < 3, with the increase of the NSST decomposition scale, the boundary and texture features of the image are gradually obvious, and the detailed information is enhanced. When 5 > j > 3, the enhancement effect is further improved; the change is not significant.

IV. RESULT ANALYSIS

To demonstrate the effectiveness of the proposed algorithm, experiments were conducted on six x-ray images collected from the website http://acm.cs.nctu.edu.tw/. For all the images, the enhanced images are obtained and are compared with existing method. Further, average gradient (AG), Image entropy (H), Spatial Frequency (SF) and Edge Intensity (EI) is evaluated for all the input images for both existing and proposed methods, which are presented in this section.

A. $Average\ Gradient\ \ (AG) = \frac{\sum_{I=1}^{M}\sum_{J=1}^{N}((f(i,j)-f(i+1,j))^2+((f(i,j)-f(i,j+1))^2)^{1/2}}{MN}$ (11)

Where

$f(i,j)$- pixel intensity at ith row and jth column

$f(i+1,j)$-- pixel intensity at i+1th row and jth column

$f(i,j+1)$-- pixel intensity at ith row and j+1th column

M-Number of rows in an image

N-number of columns in an image

AG can reflect the sharpness of the image

B. Entropy (H):

The information entropy (H) is an important indicator to measure the richness of image information and is defined as:

$$H = -\sum_{i=0}^{L-1} P_i \log P_i \quad (12)$$

P_i- Probability of occurrence of i^{th} gray value in an image

C. Spatial frequency $(SF) = \sqrt{RF^2 + CF^2}$

$$\text{Row frequency, } RF = \sqrt{\frac{1}{MN}\sum_{i=1}^{M}\sum_{j=2}^{N}\left(f(i,j) - f(i,j-1)\right)^2} \quad (13)$$

$$\text{Column Frequency, CF} = \sqrt{\frac{1}{MN}\sum_{i=2}^{M}\sum_{j=1}^{N}\left(f(i,j) - f(i-1,j)\right)^2} \quad (14)$$

Spatial frequency (SF) can reflect the overall activity of an image in the spatial domain. The higher the spatial frequency, the better is the quality of the enhanced image.

D. Edge Intensity $(EI) = \sum_{i=1}^{M}\sum_{j=1}^{N}\sqrt{G_x^2 + G_y^2}$ (15)

Where

$$G_x(i,j) = f(i,j) \times g_x$$
$$G_y(i,j) = f(i,j) \times g_y$$
$$g_x = \frac{1}{4}\begin{bmatrix} -1 & 0 & 1 \\ -2 & 0 & 2 \\ -1 & 0 & 1 \end{bmatrix}$$
$$g_y = \frac{1}{4}\begin{bmatrix} -1 & -2 & 1 \\ 0 & 0 & 0 \\ 1 & 2 & 1 \end{bmatrix}$$

The edge intensity (EI) reflects the image clarity degree. The more abundant the image detail and edge is the higher the image clarity.

.

The input images considered for image enhancement are presented in figure 5. An X-ray image of lung captured at low illumination is presented in figure 6(a). This image subjected to enhancement using the existing Automatic Gamma Correction with Weight Distribution (AGCWD) method and proposed method based on Non-sub sampled Shearlet transform involving AGCWD and guided filtering. The image enhancement results of both existing and proposed methods are presented in (b) and (c) of figure 6. The performance metric values of these methods for the enhanced image are presented in table I.

(a) Low intensity Lung

(b) Infected Lung

(c) Infected Lung

(d) Hand image

(e) Leg Image

(f) Lena Image

Fig.5 Input X-ray images considered for testing

(a) Input Image (b) Enhanced image using Existing method (c) Enhanced image using Proposed method

Fig.6 Results of Image Enhancement of Low intensity lung image

Table I: Performance metric values of enhanced Low intensity lung image

Method	Average Gradient (AG)	Entropy (H)	Spatial Frequency (SF)	Edge Intensity (EI)
Existing	1.40	6.47	3.59	15.21
Proposed	5.82	7.48	13.22	62.60

From the results, it is clear that the proposed method of image enhancement can improve the contrast of the input image much better than the exiting method as evident from the values of AG,H, SF and EI, which are far better than the values of existing method of image enhancement.

An X-ray image of lung infected with disease is presented in figure 7(a). This image subjected to enhancement using the existing Automatic Gamma Correction with Weight Distribution (AGCWD) method and proposed method based on Non-sub sampled Shearlet transform involving AGCWD and guided filtering. The image enhancement results of both existing and proposed methods are presented in (b) and (c) of figure 7. The performance metric values of these methods for the enhanced image are presented in table II.

(a) Input Image (b) Enhanced image using Existing method (c) Enhanced image using Proposed method

Fig.7 Results of Image Enhancement of infected lung image

Table II: Performance metric values of enhanced infected lung image

Method	Average Gradient (AG)	Entropy (H)	Spatial Frequency (SF)	Edge Intensity (EI)
Existing	5.68	7.18	12.25	45.40
Proposed	7.11	7.42	14.68	68.52

From the results, it is clear that the proposed method of image enhancement can improve the contrast of the input image much better than the exiting method as evident from the values of AG,H, SF and EI, which are far better than the values of existing method of image enhancement. Hence the proposed method is more suitable to identify or diagnose the disease infected portions in an image.
An X-ray image of lung infected with disease is presented in figure 8 (a). This image subjected to enhancement using the existing Automatic Gamma Correction with Weight Distribution (AGCWD) method and proposed method based on Non-sub sampled Shearlet transform involving AGCWD and guided filtering. The image enhancement results of both existing and proposed methods are presented in (b) and (c) of figure 8. The performance metric values of these methods for the enhanced image are presented in table III.

(a) Input Image

(b) Enhanced image using Existing method

(c) Enhanced image using Proposed method

Fig.8 Results of Image Enhancement of infected lung image

Table III: Performance metric values of enhanced infected lung image

Method	Average Gradient (AG)	Entropy (H)	Spatial Frequency (SF)	Edge Intensity (EI)
Existing	4.47	7.01	9.03	19.31
Proposed	7.71	7.50	13.94	52.92

From the results, it is clear that the proposed method of image enhancement can improve the contrast of the input image much better than the exiting method as evident from the values of AG,H, SF and EI, which are far better than the values of existing method of image enhancement. Hence the proposed method is more suitable to identify or diagnose the disease infected portions in an image. Hence the proposed method is more suitable to identify or diagnose the disease infected portions in an image.
An X-ray image of lung infected with disease is presented in figure 9 (a). This image subjected to enhancement using the existing Automatic Gamma Correction with Weight Distribution (AGCWD) method and proposed method based on Non-sub sampled Shearlet transform involving AGCWD and guided filtering. The image enhancement results of both existing and proposed methods are presented in (b) and (c) of figure 9. The performance metric values of these methods for the enhanced image are presented in table IV.

(a) Input Image (b) Enhanced image using Existing method (c) Enhanced image using Proposed method

Fig.9 Results of Image Enhancement of hand image

Table IV: Performance metric values of enhanced hand image

Method	Average Gradient (AG)	Entropy (H)	Spatial Frequency (SF)	Edge Intensity (EI)
Existing	4.12	6.99	9.73	30.42
Proposed	6.07	7.43	17.22	79.34

From the results, it is clear that the proposed method of image enhancement can improve the contrast of the input image much better than the exiting method as evident from the values of AG,H, SF and EI, which are far better than the values of existing method of image enhancement. Hence the proposed method is more suitable to identify or diagnose the disease infected portions in an image. Hence the proposed method is more suitable to identify or diagnose the disease infected portions in an image.

An X-ray image of lung infected with disease is presented in figure 10 (a). This image subjected to enhancement using the existing Automatic Gamma Correction with Weight Distribution (AGCWD) method and proposed method based on Non-sub sampled Shearlet transform involving AGCWD and guided filtering. The image enhancement results of both existing and proposed methods are presented in (b) and (c) of figure 10. The performance metric values of these methods for the enhanced image are presented in table V.

(a) Input Image (b) Enhanced image using Existing method (c) Enhanced image using Proposed method

Fig.10 Results of Image Enhancement of leg image

Table V: Performance metric values of enhanced leg image

Method	Average Gradient (AG)	Entropy (H)	Spatial Frequency (SF)	Edge Intensity (EI)
Existing	4.87	7.11	13.40	51.47
Proposed	6.50	7.46	15.51	74.28

From the results, it is clear that the proposed method of image enhancement can improve the contrast of the input image much better than the exiting method as evident from the values of AG,H, SF and EI, which are far better than the values of existing method of image enhancement. Hence the proposed method is more suitable to identify or diagnose the disease infected portions in an image. Hence the proposed method is more suitable to identify or diagnose the disease infected portions in an image.

A benchmark image of called 'lena' considered for testing is presented in figure 11 (a). This image subjected to enhancement using the existing Automatic Gamma Correction with Weight Distribution (AGCWD) method and proposed method based on Non-sub sampled Shearlet transform involving AGCWD and guided filtering. The image enhancement results of both existing and proposed methods are presented in (b) and (c) of figure 11. The performance metric values of these methods for the enhanced image are presented in table VI.

(a) Input Image

(b) Enhanced image using Existing method

(c) Enhanced image using Proposed method

Fig.11 Results of Image Enhancement of Lena image

From the results, it is clear that the proposed method of image enhancement can improve the contrast of the input image much better than the exiting method as evident from the values of AG,H, SF and EI, which are far better than the values of existing method of image enhancement. Hence the proposed method is more suitable to enhance the details of the low illuminated images effectively.

Table VI: Performance metric values of enhanced Lena image

Method	Average Gradient (AG)	Entropy (H)	Spatial Frequency (SF)	Edge Intensity (EI)
Existing	21.27	7.25	32.77	50.81
Proposed	36.18	7.26	66.20	139.93

Average values of the performance metrics are calculated from the results of the six input images and are tabulated in table VII. The performance analysis of the average metrics is shown in figure 12 for existing and proposed methods with respect to original images.

Table VII: Average values of performance metrics from all six images

Method	Average Gradient (AG)	Entropy (H)	Spatial Frequency (SF)	Edge Intensity (EI)
Original	6.96	7.00	13.46	35.43
Existing	6.52	7.23	13.88	59.94
Proposed	11.56	7.42	23.47	79.59

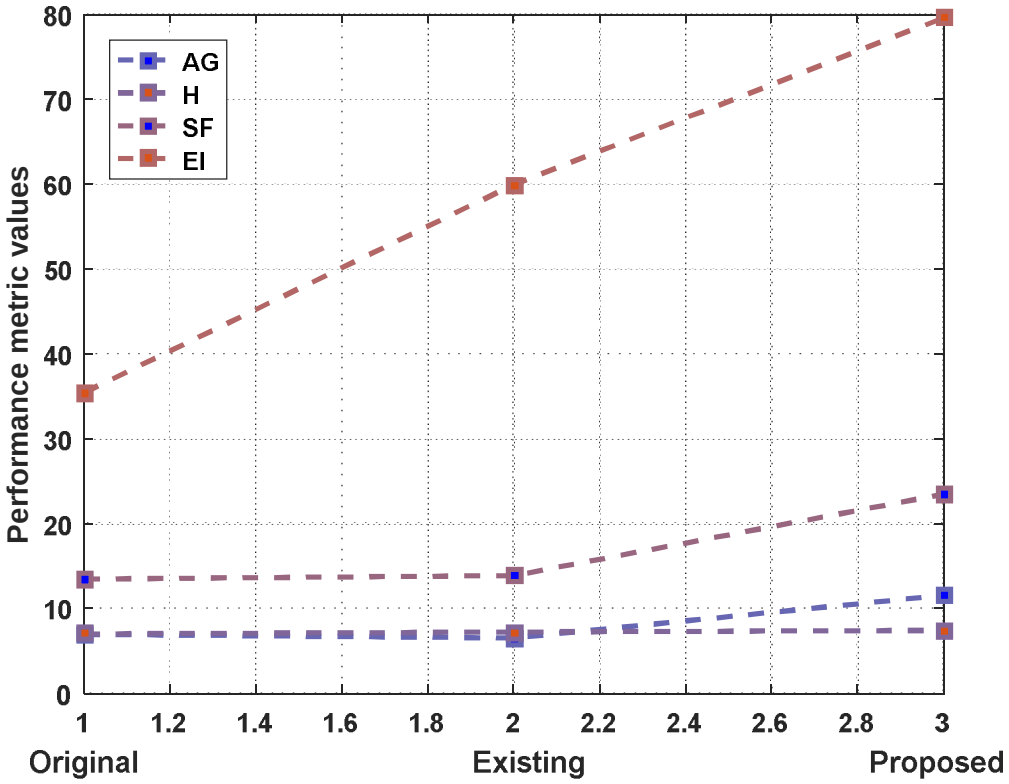

Fig.12 Comparative analysis of average performance metrics

From the comparative analysis, the proposed method performed better in terms of enhancing the quality of the input images while simultaneously reducing the distortion and noise when compared to existing method.

V. CONCLUSION

The low contrast of X-ray images makes it difficult to identify tiny and abnormal details. In order to solve this problem, a novel X-ray image enhancement method based on Non-Sub sampled Shearlet transform is proposed in this paper. The low frequency sub bands of decomposed input image after NSST is enhanced using Automatic Gamma Correction with Weight Distribution (AGCWD) technique while the directional sub bands are enhanced using gradient domain guided filtering technique. Later these bands are combined to reconstruct the enhanced image in spatial domain. The performance of the proposed image is tested on six different images in terms of average gradient (AG), Image entropy (H), Spatial Frequency (SF) and Edge Intensity (EI) and compared with existing method of image enhancement. Result analysis showed that proposed method performed better in terms of enhancing the quality of the input images while simultaneously reducing the distortion and noise when compared to existing method.

REFERENCES

[1] Zhao, Tao, and Si-Xiang Zhang. 2022. "X-ray Image Enhancement Based on Nonsubsampled Shearlet Transform and Gradient Domain Guided Filtering" Sensors 22, no. 11: 4074. https://doi.org/10.3390/s22114074.

[2] Yang, Y., Su, Z. and Sun, L., “Medical image enhancement algorithm based on wavelet transform”, IET Electronics Letters, Sun L. Medical image enhancement algorithm based on wavelet transform, Vol. 46, No. 2, pp. 120-121, 2010.

[3] Li Yang, Yanmei Liang and Hailun Fan, “Study on the methods of image enhancement for liver CT images”, Optik - International Journal for Light and Electron Optics, Vol. 121, No 19, pp.1752-1755, 2010.

[4] Peng Feng, Yingjun Pan, Biao Wei and Wei Jin Deling Mi, “Enhancing Retinal Image by the Contourlet Transform”, Pattern Recognition Letters, Vol. 28, No. 4, pp. 516-522, 2007.

[5] Sundaram M., Ramar K., Arumugam N. and Prabin G. “Histogram Modified Local Contrast Enhancement for mammogram images”, Applied Soft Computing, Vol. 11, No. 8, pp. 5809-5816, 2011.

[6] Tay, P.C., Garson, C.D., Acton, S.T. and Hossack, J.A. "Ultrasound Despeckling for Contrast Enhancement", IEEE Transactions on Image Processing, Vol. 19, No. 7, pp. 1847-1860, 2010.
[7] Bhutada, G.G., Anand, R.S. and Saxena, S.C., "Edge preserved image enhancement using adaptive fusion of Images Denoised by Wavelet and Curvelet Transform", Digital Signal Processing, Vol. 21, No.1, pp.118-130, 2011.
[8] Karen F. Panetta, Yicong Zhou, Sos Agaian and Hongwei Jia, "Nonlinear Unsharp Masking for Mammogram Enhancement", IEEE Transactions on Information Technology in Biomedicine, Vol. 15, No.6, pp.918-928, 2011.
[9] Zhiguo Gui and Yi Liu, "An Image Sharpening Algorithm based on Fuzzy Logic", International Journal for Light and Electron Optics, Vol. 122, pp. 697-702, 2011.
[10] Eltoukhy, M. M., Faye, I. and Samir, B.B., "Breast cancer diagnosis in digital mammogram using multiscale curvelet transform", 171 Computerized Medical Imaging and Graphics. Vol. 34, No.4, pp. 269-276, 2010.
[11] Phan, T. H. Truc, Md. A. U. Khan, Young-Koo Lee, Sungyoung Lee and Tae-Seong Kim, "Vessel Enhancement Filter Using Directional Filter Bank", Computer Vision and Image Understanding, Vol.113, pp. 101-112, 2009.
[12] Akram, M. U., Atzaz, A., Aneeque, S. F. and Khan, S. A., "Blood Vessel Enhancement and Segmentation using Wavelet Transform", IEEE International Conference on Digital Image Processing, pp. 34-38, 2009.
[13] Louis D.N., Ohgaki H., Wiestler O.D, Cavenee W.K. (Eds.), "WHO Classification of Tumors of the Central Nervous System", International Agency for Research on Cancer (IARC), Lyon, France, 2007.
[14] Jan C. Buckner, "Central Nervous System Tumors", Mayo Clinic Proceedings, Vol. 82, No. 10, pp. 1271-1286. 2007.
[15] Vidyarthi, Mittal, "Probabilistic mutual information based extraction of malignant brain tumors in MR images", 9th IEEE International Conference on Industrial and Information Systems (ICIIS), pp. 1-6, 2014.
[16] Shabana Urooj , Amir, "An Automated Approach of CT Scan Image Processing for Brain Tumor Identification and Evaluation", Journal of Advances in Biomedical Engineering and Technology, vol.2, pp. 11-16, 2015.
[17] R.C. Gonzalez and R.E. Woods, Digital Image Processing: 3rd ed., 2008, Pearson Education Inc.
[18] A. Beghdadi and A. L. Négrate, "Contrast enhancement technique based on local detection of edges," Computer Vision, Graphics, and Image Processing, Vol. 46, No. 2, pp. 162–174, 1989.
[19] Robert H. Sherrier and G. A. Johnson, "Regionally Adaptive Histogram Equalization of the Chest", IEEE Transactions on Medical Imaging, Vol. 6, No. 1, pp. 1 -7, 1987.
[20] Andrea Polesel, Giovanni Ramponi, and V. John Mathews, "Image Enhancement via Adaptive Unsharp Masking", IEEE Transactions on Image Processing, Vol. 9, No. 3, pp. 505 – 510, 2000.
[21] Jean-Luc Starck, Fionn Murtagh, Emmanuel J. Candès, and David L. Donoho, "Gray and Color Image Contrast Enhancement by the Curvelet Transform", IEEE Transactions on Image Processing, Vol. 12, No. 6, pp. 706 – 717, 2003.
[22] Huang Kaiqi, Wu Zhenyang and Wang Qiao, "Image enhancement based on the statistics of visual representation", Image and Vision Computing, Vol. 23, No.1, pp. 51–57, 2005.
[23] Nagesha and G. Hemantha Kumar, "A level crossing enhancement scheme for chest radiograph images", Computers in Biology and Medicine, Vol. 37, No. 10, pp. 1455 – 1460, 2007.
[24] Aditi Majumder and Sandy Irani, "Perception-Based Contrast Enhancement of Images", ACM Transactions on Applied Perception, Vol. 4, No. 3, Article 17, 2007.
[25] Sos S. Agaian, Blair Silver and Karen A. Panetta, "Transform Coefficient Histogram-Based Image Enhancement Algorithms Using 164 Contrast Entropy", IEEE Transactions on Image Processing, Vol. 16, No. 3, pp. 741 – 758, 2007.
[26] Buyue Zhang and Jan P. Allebach, "Adaptive Bilateral Filter for Sharpness Enhancement and Noise Removal", IEEE Transactions on Image Processing, Vol. 17, No. 5, pp. 664 – 678, 2008.
[27] T.L. Economopoulos, P.A. Asvestas and G.K. Matsopoulos, "Contrast enhancement of images using Partitioned Iterated Function Systems", Image and Vision Computing, Vol. 28, No. 1, pp. 45–54, 2010.
[28] D.H. Kim and E.Y. Cha, "Intensity surface stretching technique for contrast enhancement of digital photography", Multidimensional Systems and Signal Processing, Vol. 20, No. 1, pp. 81 – 95, 2009.
[29] H. Huang and X. Xiao, "Example-based contrast enhancement by gradient mapping", Visual Computer, Vol. 26, No. 6-8, pp. 731–738, 2010.
[30] Chi-Yi Tsai and Chien-Hsing Chou, "A novel simultaneous dynamic range compression and local contrast enhancement algorithm for digital video cameras", EURASIP Journal on Image and Video Processing, Vol. 2011, No. 6, pp. 1 – 19, 2011.
[31] John B. Zimmerman, Stephen M. Pizer, Edward V. Staab, J. Randolph Perry, William Mccartney and Bradley C. Brenton, "An Evaluation of the Effectiveness of Adaptive Histogram Equalization for Contrast Enhancement", IEEE Transactions on Medical Imaging, Vol. 7, No. 4, pp. 304 – 312, 1988.
[32] Y. T. Kim, "Contrast Enhancement Using Brightness Preserving BiHistogram Equalization", IEEE Transactions on Consumer Electronics, Vol. 43, No. 1, pp. 1 – 8, 1997.
[33] Yu Wang, Qian Chen and Baomin Zhang, "Image Enhancement Based on Equal Area Dualistic Sub-Image Histogram Equalization Method", IEEE Transactions on Consumer Electronics, Vol. 45, No. 1, pp. 68 –75, 1999.
[34] JC. Fu, H.C. Lien and S.T.C. Wong, "Wavelet-based histogram equalization enhancement of gastric sonogram images", Computerized Medical Imaging and Graphics, Vol. 24, No. 2, pp. 59 – 68, 2000.
[35] Sarif Kumar Naik and C. A. Murthy, "Hue-Preserving Color Image Enhancement Without Gamut Problem", IEEE Transactions On Image Processing, Vol. 12, No. 12, pp. 1591 – 1598, 2003.
[36] Chang-Jiang Zhang and Min Hu, "Contrast enhancement for image by WNN and GA combining PSNR with information entropy", Fuzzy Information and Engineering - Advances in Soft Computing, Vol. 40,pp. 3 - 15, 2007.
[37] Rui,W.; Guoyu,W. Medical X-Ray Image Enhancement Method Based on TV-Homomorphic Filter. In Proceedings of the 2017, 2nd International Conference on Image, Vision and Computing (ICIVC), Chengdu, China, 2–4 June 2017; pp. 315–318.
[38] Wang, X.; Chen, L. Contrast enhancement using feature-preserving bi-histogram equalization. Signal Image Video Process. 2018, 12, 685–692.

[39] Wu, W.; Yang, X.; Li, H.; Liu, K.; Jian, L.; Zhou, Z. A novel scheme for infrared image enhancement by using weighted least squares filter and fuzzy plateau histogram equalization. Multimed. Tools Appl. 2017, 76, 24789–24817.
[40] Xiao, B.; Tang, H.; Jiang, Y.; Li, W.; Wang, G. Brightness and contrast controllable image enhancement based on histogram specification. Neurocomputing 2018, 275, 2798–2809.
[41] Lombardo, P.; Oliver, C.J.; Pellizzeri, T.M.; Meloni, M. A newmaximum-likelihood joint segmentation technique for multitemporal SAR and multiband optical images. IEEE Trans. Geosci. Remote Sens. 2003, 41, 2500–2518.
[42] Magudeeswaran, V.; Ravichandran, C.; Thirumurugan, P. Brightness preserving bi-level fuzzy histogram equalization for MRI brain image contrast enhancement. Int. J. Imaging Syst. Technol. 2017, 27, 153–161.
[43] Mohan, S.; Ravishankar, M. Modified contrast limited adaptive histogram equalization based on local contrast enhancement for mammogram images. In Proceedings of the International Conference on Advances in Information Technology and Mobile Communication, Bangalore, India, 27–28 April 2012; pp. 397–403.
[44] Al-Ameen, Z.; Sulong, G. Ameliorating the Dynamic Range of Magnetic Resonance Images Using a Tuned Single-Scale Retinex Algorithm. Int. J. Signal Processing Image Process. Pattern Recognit. 2016, 9, 285–292. [CrossRef]
[45] Zeng, M.; Li, Y.; Meng, Q.; Yang, T.; Liu, J. Improving histogram-based image contrast enhancement using gray-level information histogram with application to X-ray images. Optik 2012, 123, 511–520. [CrossRef]
[46] Panetta, K.; Zhou, Y.; Agaian, S.; Jia, H. Nonlinear unsharp masking for mammogram enhancement. IEEE Trans. Inf. Technol. Biomed. 2011, 15, 918–928. [CrossRef]
[47] Tao, F.; Yang, X.; Wu, W.; Liu, K.; Zhou, Z.; Liu, Y. Retinex-based image enhancement framework by using region covariance filter. Soft Comput. 2018, 22, 1399–1420.

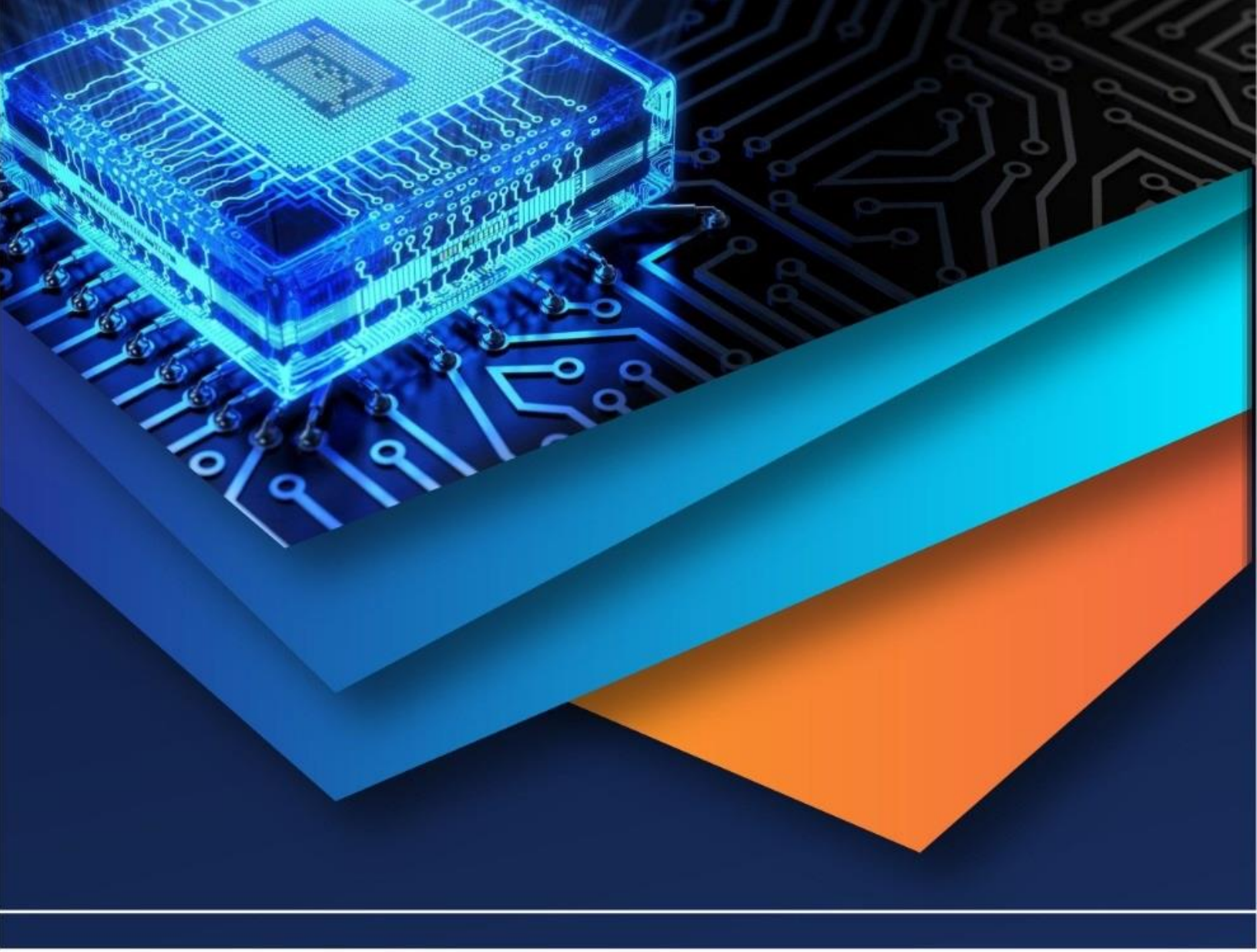

10.22214/IJRASET

45.98

IMPACT FACTOR: 7.129

IMPACT FACTOR: 7.429

INTERNATIONAL JOURNAL FOR RESEARCH

IN APPLIED SCIENCE & ENGINEERING TECHNOLOGY